RARE DISEASES

Postnatal Soluble FGFR3 Therapy Rescues Achondroplasia Symptoms and Restores Bone Growth in Mice

Stéphanie Garcia,[1,2,3] Béatrice Dirat,[1,3] Thomas Tognacci,[1,3] Nathalie Rochet,[4] Xavier Mouska,[4] Stéphanie Bonnafous,[1,3,5] Stéphanie Patouraux,[1,3,6] Albert Tran,[1,3,5] Philippe Gual,[1,3,5] Yannick Le Marchand-Brustel,[1,3] Isabelle Gennero,[7] Elvire Gouze[1,3]*

Achondroplasia is a rare genetic disease characterized by abnormal bone development, resulting in short stature. It is caused by a single point mutation in the gene coding for fibroblast growth factor receptor 3 (FGFR3), which leads to prolonged activation upon ligand binding. To prevent excessive intracellular signaling and rescue the symptoms of achondroplasia, we have developed a recombinant protein therapeutic approach using a soluble form of human FGFR3 (sFGFR3), which acts as a decoy receptor and prevents FGF from binding to mutant FGFR3. sFGFR3 was injected subcutaneously to newborn *Fgfr3*$^{ach/+}$ mice—the mouse model of achondroplasia—twice per week throughout the growth period during 3 weeks. Effective maturation of growth plate chondrocytes was restored in bones of treated mice, with a dose-dependent enhancement of skeletal growth in *Fgfr3*$^{ach/+}$ mice. This resulted in normal stature and a significant decrease in mortality and associated complications, without any evidence of toxicity. These results describe a new approach for restoring bone growth and suggest that sFGFR3 could be a potential therapy for children with achondroplasia and related disorders.

INTRODUCTION

Mutations in the gene encoding fibroblast growth factor receptor 3 (FGFR3) are responsible for the phenotypes of numerous skeletal chondrodysplasias (*1*), including achondroplasia (*2*), the most common form of short limb dwarfism. Children affected by achondroplasia suffer from abnormal long bone development, resulting in short stature. In the most severe cases, they can suffer from deformations of the skull and vertebrae that can lead to severe neurological and orthopedic complications (*3*, *4*). At present, no standard treatment can completely cure this condition. Injecting the human growth hormone or leg-lengthening surgeries have been done, but there are no clear and positive data regarding such treatments (*5*).

Achondroplasia is an autosomal dominant disorder caused by a point mutation in the gene coding for *FGFR3* (*6*). In ~97% of affected patients, achondroplasia is caused by a G380R substitution in the transmembrane domain of the receptor (*7*, *8*). This mutation results in a gain of function (*9*), which prolongs activation of the tyrosine kinase activity of the receptor (*10*, *11*). The G380R mutant FGFR3 remains ligand-dependent for its dimerization and activation (*10*, *12*); however, the presence of the mutation stabilizes the ligand/receptor complex (*13*) and slows down receptor internalization, thus extending subsequent intracellular Ras/mitogen-activated protein kinase (MAPK) pathway signaling (*10*). This FGFR3 signaling is prolonged and steadily inhibits chondrocyte proliferation and differentiation in the growth plate. Cells expressing the mutant receptor do not mature and are not replaced by mineralized bone matrix, impairing the lengthening of all bones formed by endochondral ossification (*14*). These include the long bones, as well as the vertebrae, sternum, and some cranial bones. Indeed, in the skull, bone growth can be driven by synchondroses, which are cartilaginous structures consisting of two opposed growth plates with a common zone of resting chondrocytes. As with endochondral growth plates in the long bones, synchondroses also become replaced by bone.

Despite an increasing number of studies deciphering the mechanisms responsible for bone growth disturbances, there is still no cure available for achondroplasia. Because activation of mutant FGFR3 requires ligand binding (*1*, *4*), we designed a treatment strategy based on the use of a soluble form of FGFR3 (sFGFR3). We hypothesized that sFGFR3 could act as a decoy receptor and titrate surrounding available FGFs, particularly FGF9 (*15*) and FGF18 (*16*), which are thought to be the preferential FGFR3 ligands in the growth plate chondrocytes, thus preventing their fixation on the mutant receptor. Our experiments were performed in a mouse model of achondroplasia (*Fgfr3*$^{ach/+}$) (*17*). Similar to humans, these heterozygous animals express an aberrantly activated FGFR3 containing the G380R mutation in the growth plate. They display a phenotype essentially identical to the human pathology, with shortening of all bones formed by endochondral ossification. Associated complications include upper airway obstruction, spinal cord compression, paralysis, and spinal deformities.

Here, we show that after repeated subcutaneous injections of recombinant sFGFR3 throughout the growth period, normal skeletal growth can be restored in transgenic *Fgfr3*$^{ach/+}$ mice, resulting in normal body length and significant decrease in mortality and associated complications. Moreover, no signs of short-term toxicity were detected, and treated animals were fertile and had normal offspring. These preclinical results suggest that this decoy approach may be a viable treatment for achondroplasia.

[1]INSERM, U1065, Team 8, Mediterranean Center for Molecular Medicine, 06204 Nice, France. [2]University of Paul Sabatier Toulouse III, 31062 Toulouse, France. [3]University of Nice-Sophia Antipolis, 06100 Nice, France. [4]UMR CNRS 7277, INSERM U1091, Valrose Biology Institute, University of Nice Sophia Antipolis, 06108 Nice, France. [5]Department of Digestive Diseases, University Hospital Center of l'Archet, 06202 Nice, France. [6]Department of Biology, University Hospital Center of l'Archet, 06202 Nice, France. [7]INSERM, U1043, Center of Physiopathology of Toulouse Purpan, 31024 Toulouse, France.
*Corresponding author. E-mail: elvire.gouze@inserm.fr

RESULTS

sFGFR3 increases survival of *Fgfr3*$^{ach/+}$ mice

sFGFR3 was produced by transient transfection of a plasmid encoding the FGFR3ΔTM sequence. The protein was labeled with a FLAG tag to allow for its rapid purification and detection (Fig. 1A). This tag has already been used in vivo without inducing premature elimination of the tagged protein by the immune system (*18*, *19*). Recombinant FLAG-sFGFR3 was produced by transient transfection in human embryonic kidney (HEK) 293 cells, allowing for all necessary posttranslational modifications. In mice, the half-life of sFGFR3 is 16 hours (Fig. 1B).

The biological effects of sFGFR3 were evaluated after a 3-week-long injection regimen to 3-day-old neonate mice. All newborn male and female mice from one litter received the treatment twice per week over the course of 3 weeks: sFGFR3 (0.25 or 2.5 mg/kg) (n = 76 or 104, respectively) or vehicle for control groups (n = 132). The first observation was the significant reduction in mortality with treatment: mortality for vehicle-treated *Fgfr3*$^{ach/+}$ mice was 63% compared with 20 and 12% in the low-dose (0.25 mg/kg) and high-dose (2.5 mg/kg) sFGFR3 groups, respectively (Fig. 1C) (P < 0.0001, Student's t test, significant difference from vehicle-treated *Fgfr3*$^{ach/+}$ mice). There was no significant difference between the treated groups (P = 0.9279, Student's t test).

During the 21-day treatment regimen, some *Fgfr3*$^{ach/+}$ animals died prematurely or were euthanized because of paraplegia (Fig. 1D). No wild-type animals died prematurely or suffered from paralysis (Fig. 1D). When possible, autopsy was performed and confirmed death due to respiratory failure as seen by the presence of blood within the lungs. Two animals in the vehicle-treated group (vehicle) died from bowel obstruction. Note that in the vehicle control group, most of the affected *Fgfr3*$^{ach/+}$ mice died from respiratory failure, whereas in the 2.5 mg/kg sFGFR3 treatment group, they mostly suffered from paraplegia and only one had respiratory distress (Fig. 1D). These data indicate that, with sFGFR3 treatment, few *Fgfr3*$^{ach/+}$ animals died and the achondroplasia phenotype was less severe.

sFGFR3 restores skeletal bone growth in *Fgfr3*$^{ach/+}$ mice

At day 22 (time of weaning), all surviving animals were sacrificed, and their growth was evaluated as measurements of body weight, body length, and tail length. No statistical difference was detected between males and females (table S1) (P = 0.332 to 0.799, Student's t test), and they were considered as one group for all subsequent analyses. sFGFR3 treatment had a dose-dependent effect on overall skeletal growth (Fig. 2, A to C, and fig. S1). *Fgfr3*$^{ach/+}$ mice were, on average, 20% lighter than their wild-type littermates but gained weight when treated with sFGFR3 (Fig. 2B and table S1). Treated transgenic mice had a stature (body and tail lengths) that was not significantly different from that of vehicle-treated wild-type controls (P = 0.410, Student's t test), indicating that the initial discrepancy between vehicle-treated transgenic and wild-type mice (average body length: 133.2 ± 6.1 mm versus 117.2 ± 6.9 mm; average tail length: 71.1 ± 0.9 mm versus 62.2 ± 3.1 mm) had been corrected (Fig. 2C).

Similar growth results were obtained for long bone lengths. Humerus, femurs, and tibiae from treated *Fgfr3*$^{ach/+}$ mice were significantly longer than those from vehicle-treated transgenic mice (P < 0.05, Student's t test) and reached the length of normal (vehicle-treated) wild-type bones (Fig. 2C). sFGFR3 treatment also caused growth of the long bones in wild-type mice. Micro–computed tomography (μCT) analysis of the femurs increased cortical bone thickness in treated *Fgfr3*$^{ach/+}$ mice compared to vehicle-treated wild-type animals (fig. S2). There were no differences between all groups in trabecular bone thickness (P = 0.112 to 0.750, Student's t test).

In treated *Fgfr3*$^{ach/+}$ mice, the recombinant sFGFR3 was detected within the matrix showing that the protein could penetrate the dense cartilaginous matrix of the growth plate and reach target chondrocytes (Fig. 2D). Histology confirmed sFGFR3 treatment effect on chondrocyte maturation (Fig. 2E). Treated *Fgfr3*$^{ach/+}$ mice exhibited hypertrophic chondrocytes

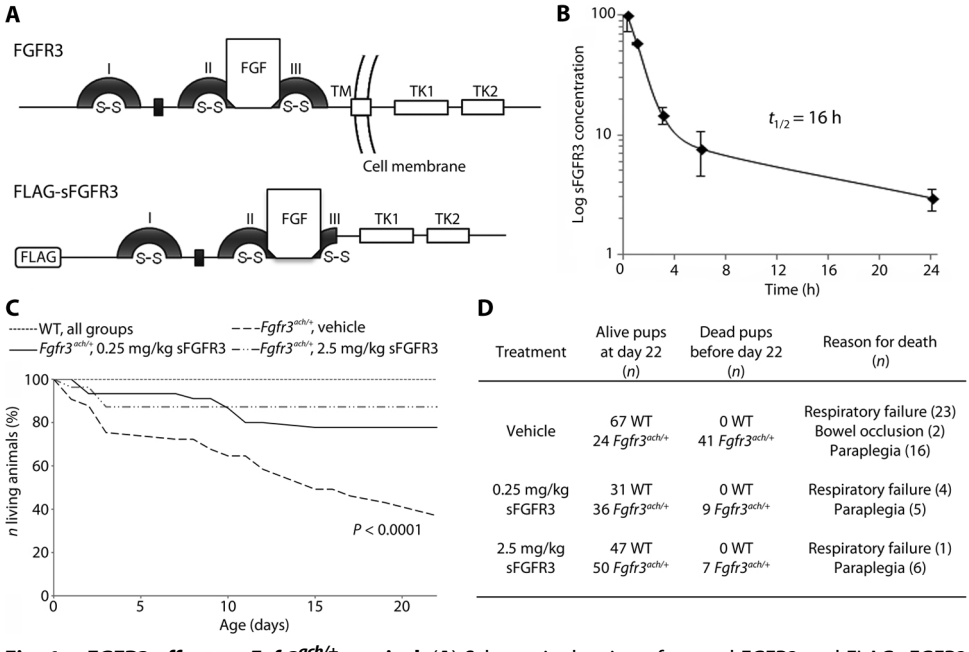

Treatment	Alive pups at day 22 (*n*)	Dead pups before day 22 (*n*)	Reason for death (*n*)
Vehicle	67 WT 24 *Fgfr3*$^{ach/+}$	0 WT 41 *Fgfr3*$^{ach/+}$	Respiratory failure (23) Bowel occlusion (2) Paraplegia (16)
0.25 mg/kg sFGFR3	31 WT 36 *Fgfr3*$^{ach/+}$	0 WT 9 *Fgfr3*$^{ach/+}$	Respiratory failure (4) Paraplegia (5)
2.5 mg/kg sFGFR3	47 WT 50 *Fgfr3*$^{ach/+}$	0 WT 7 *Fgfr3*$^{ach/+}$	Respiratory failure (1) Paraplegia (6)

Fig. 1. sFGFR3 effect on *Fgfr3*$^{ach/+}$ survival. (**A**) Schematic drawing of normal FGFR3 and FLAG-sFGFR3 proteins with FGF binding. The FGFR3 protein contains three extracellular immunoglobulin (Ig) domains (I, II, and III), a transmembrane domain (TM), and two tyrosine kinases (TK1 and TK2). The N-terminal FLAG-tagged sFGFR3 lacks the C-terminal half of IgIII and the transmembrane domain (*28*). (**B**) Half-life of FLAG-sFGFR3. (**C**) Survival curve showing the percentage of living animals for each genotype in the different treatment groups over time. WT, wild type. (**D**) Number of pups in the different treatment groups at days 3 and 22. Litters were considered as single entities, and all newborn mice from the same cage received the same treatment. Dead and alive animals were counted daily. Autopsy revealed death mostly by respiratory failure and by bowel occlusion for only two animals. Animals with paraplegia were euthanized upon discovery and recorded in the dead animal group. All dead animals were *Fgfr3*$^{ach/+}$. Statistical comparison versus vehicle-treated control group was done using the Kruskal-Wallis test.

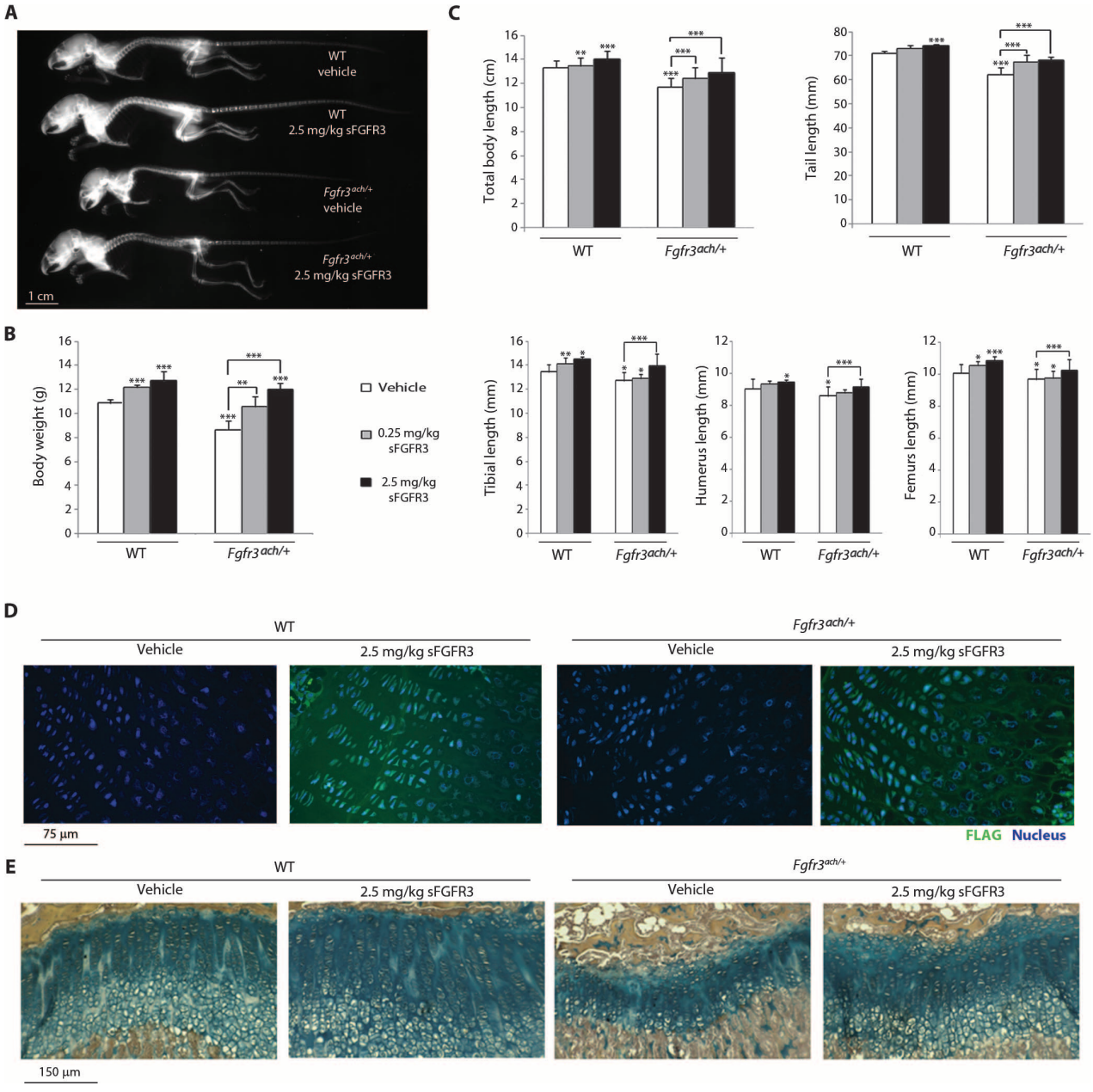

Fig. 2. sFGFR3 treatment improves overall skeletal growth. (**A**) X-ray radiographs illustrating treatment effect on skeletal growth. Shown skeletons are representative of WT and *Fgfr3*$^{ach/+}$ mice that received subcutaneous injection of vehicle or sFGFR3 (2.5 mg/kg). All data are shown in fig. S1. (**B** and **C**) Growth was characterized by body weight (B), body and tail lengths (C), and long bone measurements (C). Data followed normal distribution. **P* < 0.05, ***P* < 0.01, ****P* < 0.001 versus vehicle-treated WT, unless otherwise shown, Student's *t* test. *n* per group are shown in Table 1. (**D**) Immunohistochemical staining of FLAG-sFGFR3 in treated and vehicle-treated *Fgfr3*$^{ach/+}$ mice femoral growth plates. (**E**) Histological analysis showed organized and hypertrophic chondrocytes in the growth plate of treated *Fgfr3*$^{ach/+}$ animals. Paraffin-embedded sections were stained with Alcian blue for cartilage and Alizarin red for mineralized bone matrix. Images are representative of 10 growth plates.

in their growth plates similarly to vehicle-treated wild-type mice, which appeared to synthesize more extracellular matrix compared to vehicle-treated *Fgfr3*$^{ach/+}$ mice, as seen by the increase in growth plate cartilage.

sFGFR3 treatment also corrected rib cage development in *Fgfr3*$^{ach/+}$ mice (Fig. 3A). After chronic subcutaneous administration of sFGFR3 to neonate *Fgfr3*$^{ach/+}$ mice, normal bone growth was restored. *Fgfr3*$^{ach/+}$ and wild-type mice treated with sFGFR3 (2.5 mg/kg) showed greater sternum ossification and lengths compared with vehicle-treated animals in their respective groups (Fig. 3, B and C).

sFGFR3 treatment decreases spinal and skull deformities associated with achondroplasia

In *Fgfr3*$^{ach/+}$ mice, spinal abnormalities are recognized by the presence of a kyphosis that can be characterized by the calculation of a

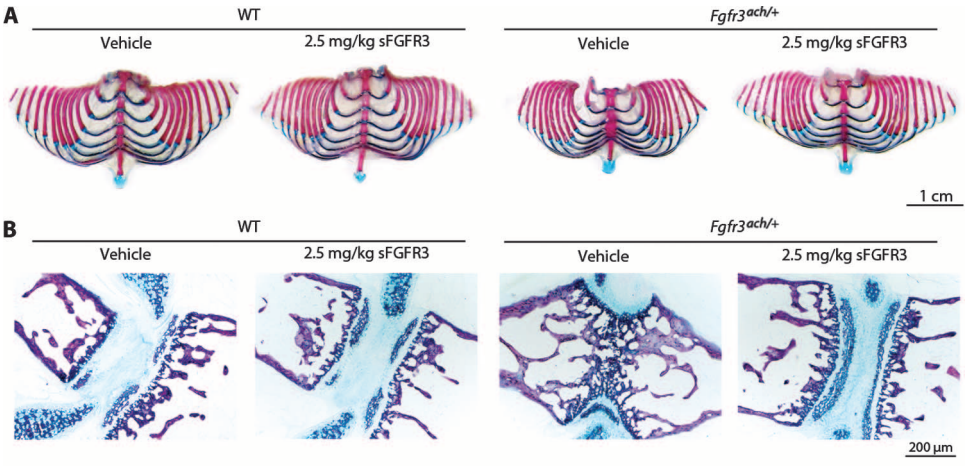

C

	Treatment	Sternum length (mm)	n
WT	Vehicle	1.72 ± 0.10	67
	0.25 mg/kg sFGFR3	1.83 ± 0.05	31
	2.5 mg/kg sFGFR3	1.87 ± 0.09*	47
Fgfr3$^{ach/+}$	Vehicle	1.33 ± 0.25 **	24
	0.25 mg/kg sFGFR3	1.64 ± 0.11 ***	36
	2.5 mg/kg sFGFR3	1.82 ± 0.09 *	50

Fig. 3. Effect of sFGFR3 treatment on rib cage development. (**A**) Representative images of rib cages stained with Alcian blue (cartilage) and Alizarin red (bone). (**B**) Histological analysis of sternum showing increased ossification in treated *Fgfr3*$^{ach/+}$ animals. Paraffin-embedded sections were stained with Alcian blue for cartilage and Alizarin red for mineralized bone matrix. (**C**) Sternum lengths. Data are means ± SD (n = 24 to 67). Data followed normal distribution. *P < 0.05, **P < 0.01, ***P < 0.001 versus vehicle-treated WT, unless otherwise noted, Student's t test.

kyphotic index (KI). In this scoring system (*20*), the KI is calculated as the ratio of length to depth of the thoracodorsal kyphosis (Fig. 4A). Length is measured as the linear distance from the ventral surface of the vertebral bodies of C7 to L6. Depth is measured as the maximum perpendicular distance from that line to the dorsal vertebral border. Smaller KI is indicative of greater kyphosis. In our study, no wild-type animals presented a spinal deformity, but 80% of vehicle-treated *Fgfr3*$^{ach/+}$ mice (n = 65) displayed kyphosis, with an average KI of 3.46 ± 0.65 (Fig. 4A). With sFGFR3 treatment, the number of *Fgfr3*$^{ach/+}$ mice with kyphosis decreased significantly to 17 and 6% in the 0.25 and 2.5 mg/kg groups, respectively (P < 0.01, Mann-Whitney test).

To further characterize vertebral maturation, we analyzed ossification of the 7th cervical (C7) and the 11th thoracic (T11). None (0%) of the wild-type animals presented immature vertebrae (Fig. 4B). In vehicle-treated *Fgfr3*$^{ach/+}$ mice, C7 and T11 were not fused at the midline in 89 and 70% of the mice, respectively (Fig. 4B). After treatment, maturation was restored to a great extent, as seen by the significant decrease in the percentage of *Fgfr3*$^{ach/+}$ mice with immature vertebrae compared with vehicle-treated animals (P < 0.05, Kruskal-Wallis test). In the 2.5 mg/kg sFGFR3 treatment group, 0% of animals had immature T11 and only 40% had immature C7. In vehicle-treated *Fgfr3*$^{ach/+}$ mice, lumbar compression characterized by paraplegia (hindlimb paralysis and bladder dysfunction) was also observed in 59% of the mice. This was improved by treatment, with only 17% of mice showing signs of lumbar compression in the 2.5 mg/kg group (Fig. 4B).

sFGFR3 treatment also prevented the premature closure of cranial synchondrosis typically observed in *Fgfr3*$^{ach/+}$ mice (Fig. 4C). Skull width (W) was not statistically different between transgenic and wild-type mice (10.3 ± 0.3 mm versus 10.2 ± 0.3 mm, respectively) (P = 0.485, Student's t test), but the length (L) was significantly shorter in *Fgfr3*$^{ach/+}$ mice (18.1 ± 0.7 mm) compared with wild-type mice (20.1 ± 0.5 mm) (P = 0.038, Student's t test) (Fig. 4C). This led to significant differences in the L/W ratio in vehicle-treated *Fgfr3*$^{ach/+}$ mice and control wild-type mice (Fig. 4C). Although no effect was observed on skull width, sFGFR3 treatment corrected the skull length, leading to similar L/W ratios in the 2.5 mg/kg–treated group and in the vehicle-treated wild-type group (P = 0.190, Student's t test) (Fig. 4C).

No toxicity signs are detected in treated animals

Because a systemic approach was used to deliver recombinant sFGFR3, we investigated possible adverse effects. Organs were analyzed in each mouse; biochemical and numeration blood tests were performed; fertility of some treated animals (two litters per group) and the normality of their offspring were verified.

Potential side effects were evaluated in liver, lung, heart, spleen, and kidneys at the time of sacrifice. None of the 255 animals that received chronic subcutaneous injections of sFGFR3 or vehicle presented macroscopic abnormalities. No signs of toxicity were observed in any histological slides (fig. S3A). Four days after the last injection of sFGFR3, traces of recombinant protein were detected only in the kidneys (fig. S3B). In all groups, organ weight changes correlated with changes in total body weight (table S2), suggesting no direct effect of sFGFR3 treatment on organ growth. Biochemical blood tests, including electrolyte titration and liver, kidney, and spleen enzymatic assays, showed normal organ function in all treated and vehicle-treated *Fgfr3*$^{ach/+}$ and wild-type animals (table S3). Blood counts were normal for all animals in this study (table S4) and remained normal for at least 8 months after treatment (table S5).

To evaluate unwanted side effects on fecundity, we weaned the animals after the 3-week treatment and mated them at 8 weeks of age with wild-type males or females. All treated animals were fertile, and their offspring had, according to their genotypes, body weights and lengths comparable to those of untreated wild-type and *Fgfr3*$^{ach/+}$ mice (Table 1). We noticed that whereas the first litters of untreated *Fgfr3*$^{ach/+}$ females were slightly reduced in size compared to those of wild-type females, the litters of primiparous treated transgenic females were identical in size to wild-type primiparous females (P = 0.345, Student's t test), confirming enlargement of their pelvic bones after treatment (Table 1).

sFGFR3 binds FGF2, FGF9, and FGF18, decreasing FGFR3 signaling in chondrocytes

To confirm the mechanism of action of sFGFR3 acting as a decoy FGFR, we first verified that sFGFR3 effectively bound free growth

A

Kyphotic index KI = [AB]/[CD]

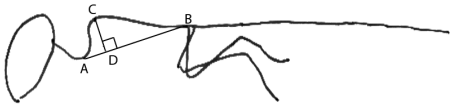

	Treatment	KI	Animals with kyphosis (KI < 4) (%)
WT	Vehicle	4.66 ± 0.72	0
	0.25 mg/kg sFGFR3	5.39 ± 0.55	0
	2.5 mg/kg sFGFR3	4.85 ± 0.64	0
***Fgfr3*$^{ach/+}$**	Vehicle	3.46 ± 0.65 *	80 *** **
	0.25 mg/kg sFGFR3	4.34 ± 0.71 *	17 * ***
	2.5 mg/kg sFGFR3	4.71 ± 0.68	6

B

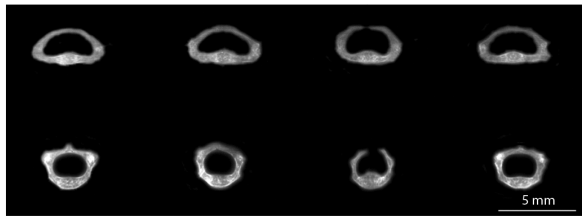

	Treatment	Immature C7 (%)	Immature T11 (%)	Lumbar compression (%)
WT	All groups	0	0	0
***Fgfr3*$^{ach/+}$**	Vehicle	89 *** **	70 *** **	59 ** **
	0.25 mg/kg sFGFR3	29 ** **	29 ** **	18 ** **
	2.5 mg/kg sFGFR3	40 **	0	17 **

C

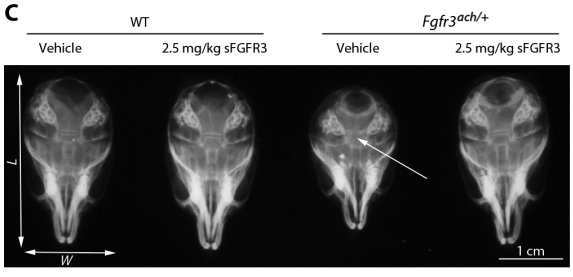

	Treatment	Width (mm)	Length (mm)	Ratio *L*/*W*
WT	Vehicle	10.3 ± 0.2	20.0 ± 0.5	1.94 ± 0.05
	0.25 mg/kg sFGFR3	10.5 ± 0.3	20.2 ± 0.4	1.93 ± 0.05
	2.5 mg/kg sFGFR3	10.6 ± 0.2	20.6 ± 0.8	1.96 ± 0.07
***Fgfr3*$^{ach/+}$**	Vehicle	10.1 ± 0.3	17.6 ± 0.6**	1.75 ± 0.07 ***
	0.25 mg/kg sFGFR3	10.1 ± 0.3	17.9 ± 0.7** *	1.77 ± 0.09 *
	2.5 mg/kg sFGFR3	10.3 ± 0.4	18.7 ± 0.7	1.81 ± 0.09

Fig. 4. Effect of sFGFR3 treatment on vertebrae maturation and skull development. (**A**) The KI (*20*) was measured from radiographs of mice positioned in right lateral recumbency. Line AB is the length of a line drawn from posterior edge of C7 to the posterior edge of L6. Line CD is the distance from line AB to the dorsal border of the vertebral body farthest from that line. Clinically, a kyphosis is characterized with KI <4. (**B**) Representative radiographs of vertebrae from vehicle-treated WT, vehicle-treated *Fgfr3*$^{ach/+}$ mice, and WT and transgenic mice receiving sFGFR3 (2.5 mg/kg). The percentage of animals with immature C7 and T11 are provided. Lumbar compressions were characterized by paraplegia or locomotion deficiency. (**C**) Representative x-rays of skulls from WT and *Fgfr3*$^{ach/+}$ mice that received either vehicle or sFGFR3 (2.5 mg/kg). Premature closure typically observed on *Fgfr3*$^{ach/+}$ mice is indicated by the arrow. Skull length (*L*) and width (*W*) were measured on the skull radiographs, and the ratio *L*/*W* was calculated. Data are means ± SD (n = 24 to 67). All data followed normal distribution. *P < 0.05, **P < 0.01, ***P < 0.001 versus vehicle-treated WT, unless otherwise noted, Student's t test.

factors. Human FGF2 (hFGF2), FGF9 (hFGF9), or FGF18 (hFGF9) or mouse FGF2 (mFGF2) was incubated with increasing quantities of sFGFR3. sFGFR3 effectively bound hFGF2, mFGF2, hFGF9, and hFGF18 in a receptor dose–dependent manner (Fig. 5A). Linear regression analysis showed no statistical differences between the four slopes (P = 0.102). Although the FGFR3ΔTM sequence used is of human origin, it could also bind mFGF2, as expected, owing to 90% sequence homology with human FGFR3. sFGFR3 competed for hFGF2 binding with endogenous FGFR3 on murine chondrocytes (ATDC5 cells), demonstrating the decoy receptor mechanism (Fig. 5B). The binding of FGF2, FGF9, or FGF18 with sFGFR3 resulted in decreased phosphorylation of FGFR and extracellular signal–regulated kinase (ERK) in chondrocytes isolated from *Fgfr3*$^{ach/+}$ mice (Fig. 5, C and D), suggesting a direct effect of sFGFR3 on intracellular FGF signaling. A soluble tumor necrosis factor (TNF) decoy receptor was used as a control protein and was unable to prevent FGF binding and effects, indicating that the results obtained with sFGFR3 are specific.

sFGFR3 treatment also restored proliferation and differentiation of mouse ATDC5 cells (Fig. 5, E and F) and significantly increased *collagen type 2*, *collagen type 10*, and *Sox9* gene expression relative to FGF alone (Fig. 5G) (P < 0.05, Student's t test). No effect on proliferation, differentiation, or gene expression was observed in the presence of the control protein.

FGF-independent mechanisms have also been explored. Signal transducer and activator of transcription 1 (Stat1) was not phosphorylated in *Fgfr3*$^{ach/+}$ chondrocytes treated with sFGFR3 (Fig. 5C). Moreover, *fgfr3* gene expression was unchanged from FGF-only controls by sFGFR3 treatment in chondrocytes isolated from *Fgfr3*$^{ach/+}$ animals (Fig. 5G). Together, these data suggest that sFGFR3 effects are mediated only through FGF-dependent pathways.

DISCUSSION

This study is a proof of concept that sFGFR3, acting as a decoy FGFR, can prevent abnormal bone growth in mice carrying the G380R achondroplasia mutation. These effects were dose-dependent: sFGFR3 (0.25 mg/kg) was sufficient to increase body weight and length in *Fgfr3*$^{ach/+}$ mice to match those of vehicle-treated wild-type mice, and

Table 1. sFGFR3 treatment did not affect fertility of the treated mice. Pups from two litters per group were weaned after 3 weeks of treatment. They were mated at 8 weeks of age with wild-type (WT) animals. The number of pups of the first litters was counted for each primiparous female. The number of WT and *Fgfr3*$^{ach/+}$ pups per litter was determined (*n* in %). At age 22 days, animals were euthanized and their body growth was evaluated. Data are means ± SD. ***P* < 0.01, ****P* < 0.001 versus untreated WT animals generated from control genitors.

Genitors	♂ × ♀	Litter size (*n* animals)	WT and *Fgfr3*$^{ach/+}$ pups per litter	Offspring body weight (g)	Offspring body length (mm)
Untreated	*Fgfr3*$^{ach/+}$ × WT	9.2 ± 0.9	74% WT, 26% *Fgfr3*$^{ach/+}$	WT, 10.88 ± 1.62 *Fgfr3*$^{ach/+}$, 8.66 ± 1.68***	WT, 133.24 ± 6.11 *Fgfr3*$^{ach/+}$, 117.25 ± 6.96***
	WT × *Fgfr3*$^{ach/+}$	7.7 ± 0.7***	70% WT, 30% *Fgfr3*$^{ach/+}$		
Treated [sFGFR3 (2.5 mg/kg)]	Treated *Fgfr3*$^{ach/+}$ × WT	10.2 ± 1.9	66% WT, 33% *Fgfr3*$^{ach/+}$	WT, 11.37 ± 1.64 *Fgfr3*$^{ach/+}$, 8.93 ± 1.98**	WT, 131.59 ± 7.29 *Fgfr3*$^{ach/+}$, 119.53 ± 5.22***
	Treated WT × WT	9.7 ± 0.9	100% WT		
	WT × treated *Fgfr3*$^{ach/+}$	10.6 ± 1.5	56% WT, 44% *Fgfr3*$^{ach/+}$	WT, 10.94 ± 2.21 *Fgfr3*$^{ach/+}$, 8.55 ± 1.97**	WT, 133.33 ± 6.71 *Fgfr3*$^{ach/+}$, 118.73 ± 6.95***
	WT × treated WT	9.8 ± 1.9	100% WT		

at a dose of 2.5 mg/kg, treated dwarf mice were even heavier and had longer long bones than vehicle-treated wild-type animals. Although it was essential that long bone growth be restored for the sFGFR3 treatment to be effective, it was also critical to significantly affect the onset of complications owing to skeletal deformities. Indeed, the phenotype penetrance is variable, and some *Fgfr3*$^{ach/+}$ animals are severely affected. Restoration of vertebra maturation and normal closure of cranial synchondroses in treated *Fgfr3*$^{ach/+}$ mice had beneficial effects on these animals. Treated transgenic mice showed reduced paraplegia, mortality, and respiratory failure compared with untreated *Fgfr3*$^{ach/+}$ animals. The use of a soluble recombinant protein also allows for cessation of treatment if safety issues are raised and at puberty when bone growth ceases. Furthermore, our study did not reveal any toxic effect on biological markers or fertility and offspring of treated animals.

Despite the increasing number of reports studying the mechanisms underlying achondroplasia and related skeletal dysplasia, only four studies have been published showing biologic-based therapeutic strategies effectively tested in mice with chondrodysplasia. Xie *et al.* recently showed that intermittent parathyroid hormone (PTH) treatment partially rescues bone growth in mice with achondroplasia (*21*). In their study, PTH was administered subcutaneously at a dose of 100 μg/kg per day for 4 weeks after birth. Although the mechanism by which PTH affects FGFR3 intracellular signaling was not clearly established, bone growth was partially rescued in treated transgenic mice, although the PTH-treated transgenic mice remained smaller than their wild-type littermates.

Another potential therapeutic antagonist of FGFR3 signaling is the C-natriuretic peptide (CNP). Yasoda *et al.* treated transgenic mice with achondroplasia by continuous intravenous infusion of synthetic CNP for 3 weeks starting at 4 weeks of age, resulting in a 12% increase in naso-anal length (*22*). It is believed that CNP increases the width of the growth plate by accelerating growth plate activity. The major obstacle for use in human is the very short half-life of CNP, estimated to be 2.6 min in plasma (*23*). To overcome this, Lorget *et al.* recently evaluated a CNP analog with a longer half-life, allowing for daily subcutaneous injections rather than continuous infusion. At the highest dose, treatment resulted in only 5.3% increase in naso-anal length (*24*).

A recent report described the use of a new FGFR3-binding peptide that rescued the lethal phenotype and partially restored the structural distortion of growth plates in mice carrying the thanatophoric dysplasia II mutation (*25*). In that study, the effects on MAPK signaling and bone growth correction were only partial, requiring daily administration, probably due to the short half-life of the peptide (2.6 min). In our study, the effects of sFGFR3 were of higher magnitude, with complete restoration of normal stature. The half-life of sFGFR3 we have used in this study is 16 hours, which is significantly prolonged compared to the small FGFR3-binding peptide or to CNP. Indeed, only six injections (between birth and weaning) were necessary to completely restore bone growth in the treated *Fgfr3*$^{ach/+}$ mice, making the hope of a possible treatment suitable in humans.

It has been demonstrated that in the case of the G380R mutation, FGFR3 activation is ligand-dependent (*10*), but there is still no clear consensus in the literature (*26*, *27*), suggesting not one but multiple mechanisms leading to prolonged intracellular signaling. Our results rule out that in this heterologous system (human protein in mice), sFGFR3 acts through FGF ligand–independent mechanisms of FGFR3 signaling, further supporting the idea that the achondroplasia mutation requires ligand binding to be activated. However, they do not exclude the potential role of sFGFR3 on the turnover of wild-type FGFR3 or on other FGFRs. It is also possible that other mechanisms of action occur in human. Further studies will be required to determine the duration of its action as a decoy receptor for FGFR and also evaluate if phenotype and survival of animals can be further improved if sFGFR3 is administered for longer period of time.

In conclusion, this study demonstrates the viability of targeting FGFR3 in the extracellular compartment as an effective treatment to restore growth plate maturation and induce normal bone growth in achondroplasia. The absence of short-term unwanted side effects strengthens its potential use as a therapy for this and related chondrodysplasias caused by activating mutation in FGFRs. However, before moving forward to the clinics, the minimal efficacy dose, as well as a possible toxic dose, needs to be determined, and the exploration of possible long-term unwanted side effects needs to be further pursued in the same animal model. In addition, it would be necessary to determine whether sFGFR3 could be administered at

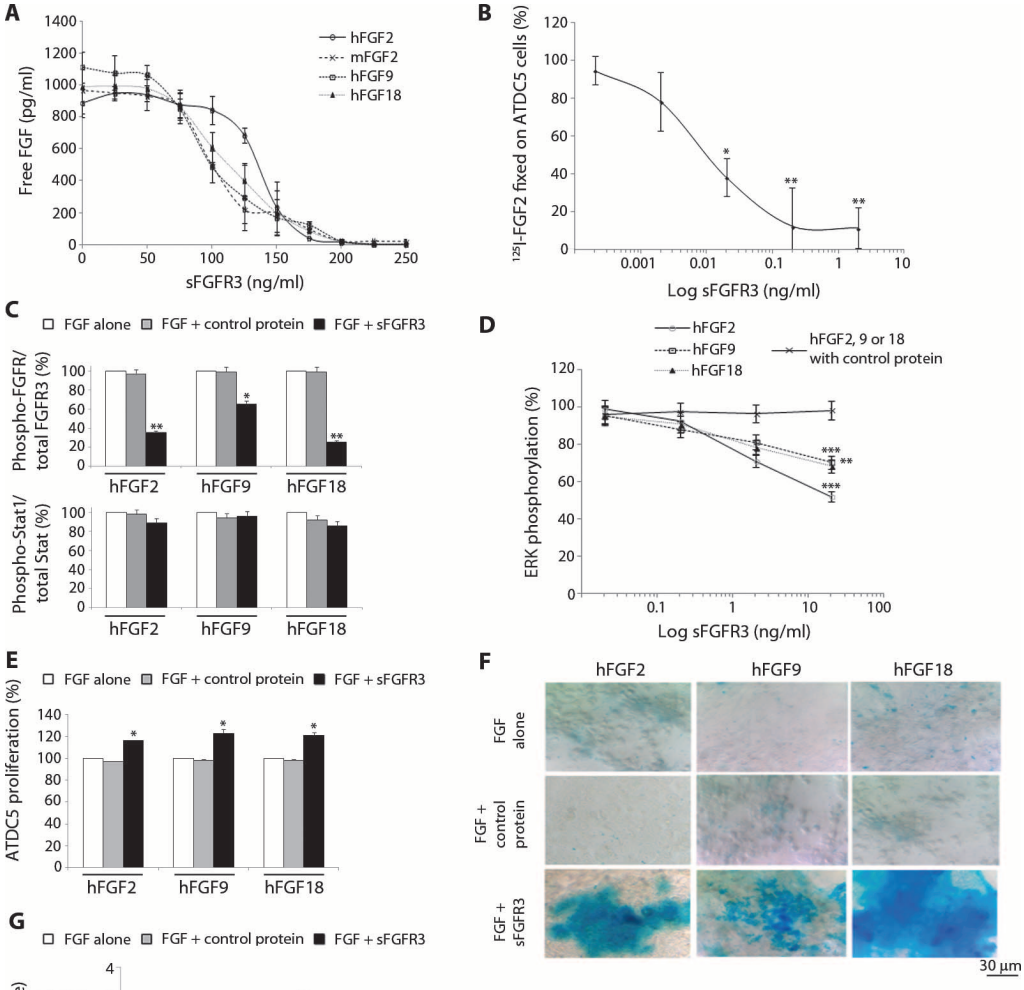

Fig. 5. sFGFR3 acts as a decoy receptor to restore chondrocyte proliferation and differentiation. (**A**) Fixed amounts of mFGF2 or hFGF2, hFGF9, or hFGF18 (100 pg/ml) were incubated with increasing concentrations of sFGFR3 (0 to 250 ng/ml). After 2 hours, unbound FGFs were detected by enzyme-linked immunosorbent assay (ELISA). (**B**) Competition binding assay showing the decrease of ^{125}I-FGF2 binding to ATDC5 cells after a 10-min challenge with increasing doses of sFGFR3 (0 to 20 ng/ml). (**C** and **D**) Phosphorylated FGFR (C), Stat1 (C), or ERK (D) on *Fgfr3*$^{ach/+}$ chondrocytes after a 10-min challenge with increasing doses of sFGFR3 (0 to 20 ng/ml) in the presence of FGF2, FGF9, or FGF18 (100 pg/ml). Results are expressed as percentage of the condition without sFGFR3. Etanercept (20 ng/ml) was used as a control in (C) and (D). (**E**) Mouse chondrocyte proliferation after 72-hour incubation in the presence of FGF2 (100 pg/ml) and sFGFR3 (0 or 20 ng/ml). Results are expressed as percentage of proliferation in the presence of FGF2 without sFGFR3. Etanercept (20 ng/ml) was used as a control. (**F**) Differentiation assay of ATDC5 cells cultured for 7 days in the presence of FGF2 (100 pg/ml) and sFGFR3 (0 or 20 ng/ml). Alcian blue stain reveals proteoglycan content. (**G**) Relative gene expression of *collagen type 2* (*Col2*), *collagen type 10* (*Col10*), *Sox9*, and endogenous *Fgfr3* in the presence of hFGF2, hFGF9, or hFGF18 (100 pg/ml) with or without sFGFR3 (20 ng/ml). Fold increase is shown versus FGF-only animals. After verification of normality, statistical comparisons were performed with a one-way analysis of variance (ANOVA) in (B) and (D), a Kruskal-Wallis test in (C), and a Student's *t* test in (E) and (F). **P* < 0.05, ***P* < 0.01, ****P* < 0.001 versus sFGFR3 (0 ng/ml). Data are means ± SD. All experiments were performed in triplicate and repeated three to five times.

later developmental stage, for example, start treatment in 1- to 2-week-old mice to, in fine, delay treatment from infancy to childhood in patients with achondroplasia.

MATERIALS AND METHODS

Study design

To prevent premature death of *Fgfr3*$^{ach/+}$ animals and rescue the symptoms of achondroplasia, we have developed a recombinant protein therapeutic approach using sFGFR3, which acts as a decoy receptor, preventing FGF from binding to mutant FGFR3. As predefined study component, we determined that our rules for stopping data collection were either premature death of the animal or sacrifice time at day 22. Because achondroplasia is a disease with an important phenotypic variability, all animals were included in the study to improve the power of the study. Animals dead before day 22 were used for the study of the impact of treatment on premature death, and animals reaching day 22 were used for all the analyses. All experiments and data measurements were performed by blinded experimenters at all times.

Two doses of sFGFR3 (0.25 and 2.5 mg/kg) were tested. At day 3, all newborn mice from a single litter received the same dose. Control litters received 10 µl of phosphate-buffered saline (PBS) containing 50% glycerol (vehicle). Thereafter, subcutaneous injections were done twice a week for 3 weeks, alternatively on the left and right sides of the back. Mice were observed daily, with particular attention to locomotion and urination alterations. Breeding was set up to theoretically generate litters with half wild-type and half heterozygous *Fgfr3*$^{ach/+}$ mice. To avoid bias due to variations of phenotype penetrance, we performed the experiments on at least two litters (one treated and one control) arising from the same breeders. A total of 15, 9, and 11 litters representing a total of 312 pups were treated with vehicle, FLAG-sFGFR3 (0.25 mg/kg), or FLAG-sFGFR3 (2.5 mg/kg), respectively. The *n* per group is presented in Fig. 1D.

At day 22, all animals but two litters per group were sacrificed by CO_2 asphyxiation. Gender was determined. All subsequent measurements and analyses were performed without knowing mice genotype to avoid any experimental bias. Genotyping was performed at the end

of the study to reveal the correspondence of data with a specific genotype. All the animals were used for all the data acquisition, except for histology and immunohistochemistry (n = 10 per group), μCT scan (n = 10 per group), fertility test (n = 9 to 12 per group), and toxicological analysis (n = 10 per group).

sFGFR3 subcloning and recombinant protein production

To facilitate subcloning, we optimized full-length complementary DNA (cDNA) sequence encoding the FGFR3ΔTM (2.1 kb) (*28*) to decrease GC content while encoding for the original protein sequence (GeneOptimizer process, GeneArt). The synthesized fragment was subcloned into pFLAG-CMV3_G727 (Sigma-Aldrich) with Hind III and Kpn I cloning sites. Plasmid DNA was purified from transformed bacteria, and concentration was determined by ultraviolet spectroscopy. The final construct was verified by sequencing.

Recombinant FLAG-sFGFR3 protein was produced by transient transfection with GeneJuice transfection reagent (Merck Millipore) in HEK 293 cells. Each transfection was performed in a cell factory (High flask T600, Merck Millipore) with 80% confluent HEK 293 in 100 ml of Dulbecco's modified Eagle's medium (DMEM) without phenol red (Life Technologies) supplemented with 2 mM glutamine (Life Technologies) and antibiotics (Life Technologies). GeneJuice (600 μl) and pFLAG-sFGFR3 (240 μg) were resuspended in 30 ml of Opti-MEM (Life Technologies), incubated 30 min at room temperature, and then incubated for 4 hours onto the cells at 37°C in 5% CO_2. Medium was then replaced by 120 ml of supplemented DMEM without phenol red. After 72 hours, production medium was filtrated with 0.22-μm filters and concentrated on Amicon Ultra-15 60-kD (Merck Millipore). Recombinant protein was then purified with an affinity column (ANTI-FLAG M2 Affinity Gel, Sigma-Aldrich) according to the manufacturer's instructions. FLAG-sFGFR3 amounts were measured by specific ELISA (R&D Systems) according to the manufacturer's instructions. FLAG-sFGFR3 was then stored at −20°C at a concentration of 0.5 μg/ml in 50% glycerol solution. Protein was stable for at least 12 months.

Animals and treatments

The *Principles of Laboratory Animal Care* (National Institutes of Health publication no. 85-23, revised 1985; http://grants1.nih.gov/grants/olaw/references/phspol.htm) and the European commission guidelines for the protection of animals used for scientific purposes (http://ec.europa.eu/environment/chemicals/lab_animals/legislation_en.htm) were followed at all times. All procedures were approved by the Institutional Ethic Committee for the Use of Laboratory Animals (CIEPAL Azur) (approval NCE-2012-52).

Experiments were performed on transgenic *Fgfr3*$^{ach/+}$ animals in which expression of the mutant FGFR3 is driven by the Col2a1 promoter/enhancer (*17*). Mice were exposed to a 12-hour light/dark cycle and had free access to standard laboratory food and water. Genotypes were verified by polymerase chain reaction (PCR) of genomic DNA with the primers 5′-AGGTGGCCTTTGACACCTACCAGG-3′ and 5′-TCTGTTGTGTTTCCTCCCTGTTGG-3′, which amplify 360 bp of the FGFR3 transgene (*17*).

Mice were treated as described in the "Study design" section. After sacrifice at day 22, body weights were measured. Blood (500 μl) was harvested by cardiac puncture and mixed with 50 μl of 0.5 M EDTA; half of the samples were centrifuged for a biochemical assessment with a Beckman AU 2700 Analyzer [electrolytes (Na^+, K^+, Cl^-), lactate dehydrogenase, cholesterol, creatinine, creatine kinase, aspartate aminotransferase (AST), alanine aminotransferase (ALT), amylase, and total bilirubin]; the other half was analyzed without centrifugation for blood numeration (Hemavet 950FS, Mascot Hematology). Cadavers were carefully skinned and eviscerated, and skeletal measurements (body and tail lengths) were obtained with an electronic digital caliper (Fisher Scientific). Total body length was measured from the nose to the end of the last caudal vertebra; tail was measured starting at the first caudal vertebra. Organs were harvested, weighed, and stored in 10% formalin for further histological analysis with standard paraffin-embedded techniques. Histology was performed on randomly selected samples from all groups, which were analyzed blindly by a pathologist (S.P.). Organs were observed for macroscopic abnormalities such as modification of color or texture and presence of nodules. Microscopically, pathology criteria included, but are not limited to, modification of organ architecture or cell morphology, presence of fibrosis, cellular dysplasia, metaplasia or atypia, and presence of inflammatory foci.

X-rays of all skeletons were taken with a Faxitron x-ray machine (Edimex). KI was measured for each animal with an established method (*20*). Femoral histomorphometric parameters (trabecular structure and cortical thickness) were determined with a μCT system (SkyScan 1173, Bruker microCT) with x-ray energy settings of 50 kV and 140 μA. Samples were scanned with an isotropic voxel size of 5.72 μm using aluminum filter of 1.0 mm and three repeated scans. The images were reconstructed with NRecon software (v1.6.4.8) with ring artifact, beam hardening, and smoothing corrections. For bone analysis, entire femurs were selected at the region of interest, and cortical thickness was measured with CTAn software (v1.13.2.0).

Cleared skeletons were then stained simultaneously with Alcian blue and Alizarin red using standard procedures and stored in glycerol before analysis. Stained long bones (tibiae, femurs, and humerus) were dissected and measured with an electronic digital caliper; rib cages were analyzed; vertebrae and skulls were then dissected and analyzed. Histological evaluations of tibial growth plate and rib cartilage were performed on paraffin-embedded sections.

Half-life of sFGFR3

To determine the half-life of sFGFR3, 8-week-old wild-type mice received an intravenous bolus of FLAG-sFGFR3 (50 mg/kg). At 15 min and 1, 3, 6, and 24 hours, blood was harvested by retro-orbital puncture with heparin catheter (n = 4). Concentration of FLAG-sFGFR3 was measured by anti-FLAG ELISA (Sigma). The half-life of the terminal phase was calculated with the following pharmacokinetic equation: $t_{1/2} = 0.693/\lambda_z$, where 0.693 is the natural logarithm of 2 and λ_z is the slope of the terminal phase (*29*).

Immunohistochemistry

At the end of the 3-week experiment, immunohistochemistry of FLAG-sFGFR3 was performed on femurs and organs of mice. Harvested tissues were fixed in 10% formalin for 24 hours. After bone decalcification in EDTA for 5 days, bones and organs were paraffin-embedded and 5-μm sections were incubated with anti-FLAG M2-FITC (fluorescein isothiocyanate) monoclonal antibody (10 μg/ml) (Sigma-Aldrich). Sections were counterstained with Hoechst solution (Sigma-Aldrich), treated with autofluorescence eliminator reagent (Merck Millipore), and visualized under fluorescence microscopy. An anti-IgG antibody (Sigma-Aldrich) was used as a negative control.

Fertility of treated animals

Animals from the litters that were not used for skeletal measurements were kept until breeding age was reached. At 8 weeks of age, they were mated with 8-week-old FVB mice from Charles River. Newborn mice were counted at birth for each treated and control male and female and compared with fertility statistics of the previous generation. At age 22, offspring were euthanized and growth was evaluated as described above.

FGF binding to sFGFR3

Fixed amounts of hFGF2 or mFGF2, hFGF9 (R&D Systems), or hFGF18 (PeproTech) were incubated for 2 hours at 37°C with increasing doses of FLAG-sFGFR3 (0 to 250 ng/ml) in PBS/1% bovine serum albumin (BSA). To verify binding specificity, etanercept (20 ng/ml) (Pfizer), a soluble TNF receptor, was used as a control. Specific commercial ELISA kits (R&D Systems; CliniSciences) were used to quantify remaining unbound FGFs. For FGF2, FGF18, and FGF9, 1000 or 1200 pg/ml was used on the basis of the sensitivity of the corresponding ELISA kits.

Proliferation and differentiation assays

sFGFR3 effect on proliferation was determined on ATDC5 cells. For this, ATDC5 cells were plated at a density of 5×10^4 in 24-well plates and cultured for 48 hours in DMEM-F12/0.5% BSA (Life Technologies). Cells were then challenged for 72 hours with FGF2, FGF9, or FGF18 (100 pg/ml) in the presence of FLAG-sFGFR3 (0 or 20 ng/ml). Proliferation was evaluated with the MTT [3-(4,5-dimethylthiazol-2-yl)-2,5-diphenyltetrazolium bromide] proliferation assay by measurement of absorbance at 540 nm.

To determine treatment effect on chondrocyte differentiation, subconfluent ATDC5 cells were incubated in 24-well plates for 7 days in chondrocyte differentiation medium [L-ascorbic acid (37.5 μg/ml), 1 mM sodium pyruvate, 1% insulin–transferrin–sodium selenite, 100 nM dexamethasone in DMEM-F12] in the presence of FGF2, FGF9, or FGF18 (100 pg/ml) and FLAG-sFGFR3 (0 or 20 ng/ml). After 7 days in culture, half of the wells were stained with Alcian blue (pH 2.5) in 3% acetic acid. In the remaining wells, total RNA was extracted with an RNeasy Mini Kit (Qiagen). Total RNA (1 μg) was reverse-transcribed, and real-time PCR was performed (ABI Prism 7500). The TaqMan gene expression assays were purchased from Applied Biosystems: *Col10a1* (Mm00487041_m1), *Col2a1* (Mm01309565_m1), *Sox9* (Mm00448840_m1), *Fgfr3* (Mm00433294_m1), and *RPLP0* (ribosomal phosphoprotein large P0, Mm00725448_s1). Gene expression values were normalized to the expression value of the housekeeping gene *RPLP0* and calculated on the basis of the comparative cycle threshold C_t method ($2^{-\Delta Ct}$) as described previously (*30*).

Statistical analysis

Statistical analyses were performed with GraphPad Prism 6.0 software. To determine the statistical tests to be used, necessary assumptions were verified. To verify normality and equal variance, an Agostino and Pearson omnibus normality test ($\alpha = 0.05$) and a Brown-Forsythe test ($P < 0.05$) were performed, respectively. Because all skeletal measurement data sets (body weight, body length, tail length, long bone length, μCT scan, sternum length, cranium length, width, and length/width) and fertility measure fulfilled normality and equal variance requirements, two-tailed Student's *t* test for comparisons of two independent groups was used in the different statistical analyses. Comparison of KI data was done with a Mann-Whitney test. Comparison of mortality data between treated and control groups, comparison of vertebrae maturation between treated and control groups, and comparison of AST and ALT between treated and control groups were done using a Kruskal-Wallis test ($P < 0.05$) with a Dunn's test. Comparison of all the other biochemical parameters and blood numeration was done using a one-way ANOVA with a Dunnett's multiple comparison test (95% confidence interval). For organ weight correlation analyses, Pearson or Spearman tests were used when data sets followed or not normal distribution, respectively ($\alpha = 0.05$). To compare correlations, a Fisher *r*-to-*z* transformation was performed. Comparison of sFGFR3 binding to human and murine FGFs was done by linear regression. In-cell Western (ICW) data distribution followed normality and was thus analyzed with a one-way ANOVA using a Holm-Sidak multiple comparisons test.

SUPPLEMENTARY MATERIALS

www.sciencetranslationalmedicine.org/cgi/content/full/5/203/203ra124/DC1

Methods

Fig. S1. Representative x-ray radiographs of skeletons of *Fgfr3*$^{ach/+}$ and wild-type mice treated with vehicle or sFGFR3.

Fig. S2. μCT analysis of femoral bone structures after sFGFR3 treatment.

Fig. S3. Histological evaluation of the organs after sFGFR3 treatment.

Table S1. Body measurements in the different treatment groups.

Table S2. Coefficient correlation (*r*) between organ and body weight in the different treatment groups.

Table S3. Blood biochemistry was unchanged by sFGFR3 treatment.

Table S4. Blood counts were not modified by sFGFR3 treatment.

Table S5. Blood counts were not modified 8 months after sFGFR3 treatment.

REFERENCES AND NOTES

1. D. M. Ornitz, FGF signaling in the developing endochondral skeleton. *Cytokine Growth Factor Rev.* **16**, 205–213 (2005).
2. W. A. Horton, G. P. Lunstrum, Fibroblast growth factor receptor 3 mutations in achondroplasia and related forms of dwarfism. *Rev. Endocr. Metab. Disord.* **3**, 381–385 (2002).
3. M. J. Wright, M. D. Irving, Clinical management of achondroplasia. *Arch. Dis. Child.* **97**, 129–134 (2012).
4. W. A. Horton, J. G. Hall, J. T. Hecht, Achondroplasia. *Lancet* **370**, 162–172 (2007).
5. E. D. Shirley, M. C. Ain, Achondroplasia: Manifestations and treatment. *J. Am. Acad. Orthop. Surg.* **17**, 231–241 (2009).
6. F. Rousseau, J. Bonaventure, L. Legeai-Mallet, A. Pelet, J. M. Rozet, P. Maroteaux, M. Le Merrer, A. Munnich, Mutations in the gene encoding fibroblast growth factor receptor-3 in achondroplasia. *Nature* **371**, 252–254 (1994).
7. G. A. Bellus, T. W. Hefferon, R. I. Ortiz de Luna, J. T. Hecht, W. A. Horton, M. Machado, I. Kaitila, I. McIntosh, C. A. Francomano, Achondroplasia is defined by recurrent G380R mutations of FGFR3. *Am. J. Hum. Genet.* **56**, 368–373 (1995).
8. R. Shiang, L. M. Thompson, Y. Z. Zhu, D. M. Church, T. J. Fielder, M. Bocian, S. T. Winokur, J. J. Wasmuth, Mutations in the transmembrane domain of FGFR3 cause the most common genetic form of dwarfism, achondroplasia. *Cell* **78**, 335–342 (1994).
9. F. Rousseau, J. Bonaventure, L. Legeai-Mallet, A. Pelet, J. M. Rozet, P. Maroteaux, M. Le Merrer, A. Munnich, Mutations of the fibroblast growth factor receptor-3 gene in achondroplasia. *Horm. Res.* **45**, 108–110 (1996).
10. E. Monsonego-Ornan, R. Adar, T. Feferman, O. Segev, A. Yayon, The transmembrane mutation G380R in fibroblast growth factor receptor 3 uncouples ligand-mediated receptor activation from down-regulation. *Mol. Cell. Biol.* **20**, 516–522 (2000).
11. D. Harada, Y. Yamanaka, K. Ueda, R. Nishimura, T. Morishima, Y. Seino, H. Tanaka, Sustained phosphorylation of mutated FGFR3 is a crucial feature of genetic dwarfism and induces apoptosis in the ATDC5 chondrogenic cell line via PLCγ-activated STAT1. *Bone* **41**, 273–281 (2007).
12. E. Monsonego-Ornan, R. Adar, E. Rom, A. Yayon, FGF receptors ubiquitylation: Dependence on tyrosine kinase activity and role in downregulation. *FEBS Lett.* **528**, 83–89 (2002).
13. M. K. Webster, D. J. Donoghue, Constitutive activation of fibroblast growth factor receptor 3 by the transmembrane domain point mutation found in achondroplasia. *EMBO J.* **15**, 520–527 (1996).
14. C. Deng, A. Wynshaw-Boris, F. Zhou, A. Kuo, P. Leder, Fibroblast growth factor receptor 3 is a negative regulator of bone growth. *Cell* **84**, 911–921 (1996).

15. S. Garofalo, M. Kliger-Spatz, J. L. Cooke, O. Wolstin, G. P. Lunstrum, S. M. Moshkovitz, W. A. Horton, A. Yayon, Skeletal dysplasia and defective chondrocyte differentiation by targeted overexpression of fibroblast growth factor 9 in transgenic mice. *J. Bone Miner. Res.* **14**, 1909–1915 (1999).
16. D. Davidson, A. Blanc, D. Filion, H. Wang, P. Plut, G. Pfeffer, M. D. Buschmann, J. E. Henderson, Fibroblast growth factor (FGF) 18 signals through FGF receptor 3 to promote chondrogenesis. *J. Biol. Chem.* **280**, 20509–20515 (2005).
17. M. C. Naski, J. S. Colvin, J. D. Coffin, D. M. Ornitz, Repression of hedgehog signaling and BMP4 expression in growth plate cartilage by fibroblast growth factor receptor 3. *Development* **125**, 4977–4988 (1998).
18. J. P. Louboutin, B. A. Reyes, L. Agrawal, E. Van Bockstaele, D. S. Strayer, Strategies for CNS-directed gene delivery: In vivo gene transfer to the brain using SV40-derived vectors. *Gene Ther.* **14**, 939–949 (2007).
19. L. R. Rodino-Klapac, C. L. Montgomery, W. G. Bremer, K. M. Shontz, V. Malik, N. Davis, S. Sprinkle, K. J. Campbell, Z. Sahenk, K. R. Clark, C. M. Walker, J. R. Mendell, L. G. Chicoine, Persistent expression of FLAG-tagged micro dystrophin in nonhuman primates following intramuscular and vascular delivery. *Mol. Ther.* **18**, 109–117 (2010).
20. N. Laws, A. Hoey, Progression of kyphosis in *mdx* mice. *J. Appl. Physiol.* **97**, 1970–1977 (2004).
21. Y. Xie, N. Su, M. Jin, H. Qi, J. Yang, C. Li, X. Du, F. Luo, B. Chen, Y. Shen, H. Huang, C. J. Xian, C. Deng, L. Chen, Intermittent PTH (1-34) injection rescues the retarded skeletal development and postnatal lethality of mice mimicking human achondroplasia and thanatophoric dysplasia. *Hum. Mol. Genet.* **21**, 3941–3955 (2012).
22. A. Yasoda, H. Kitamura, T. Fujii, E. Kondo, N. Murao, M. Miura, N. Kanamoto, Y. Komatsu, H. Arai, K. Nakao, Systemic administration of C-type natriuretic peptide as a novel therapeutic strategy for skeletal dysplasias. *Endocrinology* **150**, 3138–3144 (2009).
23. P. J. Hunt, A. M. Richards, E. A. Espiner, M. G. Nicholls, T. G. Yandle, Bioactivity and metabolism of C-type natriuretic peptide in normal man. *J. Clin. Endocrinol. Metab.* **78**, 1428–1435 (1994).
24. F. Lorget, N. Kaci, J. Peng, C. Benoist-Lasselin, E. Mugniery, T. Oppeneer, D. J. Wendt, S. M. Bell, S. Bullens, S. Bunting, L. S. Tsuruda, C. A. O'Neill, F. Di Rocco, A. Munnich, L. Legeai-Mallet, Evaluation of the therapeutic potential of a CNP analog in a *Fgfr3* mouse model recapitulating achondroplasia. *Am. J. Hum. Genet.* **91**, 1108–1114 (2012).
25. M. Jin, Y. Yu, H. Qi, Y. Xie, N. Su, X. Wang, Q. Tan, F. Luo, Y. Zhu, Q. Wang, X. Du, C. J. Xian, P. Liu, H. Huang, Y. Shen, C. X. Deng, D. Chen, L. Chen, A novel FGFR3-binding peptide inhibits FGFR3 signaling and reverses the lethal phenotype of mice mimicking human thanatophoric dysplasia. *Hum. Mol. Genet.* **21**, 5443–5455 (2012).
26. J. Placone, K. Hristova, Direct assessment of the effect of the Gly380Arg achondroplasia mutation on FGFR3 dimerization using quantitative imaging FRET. *PLoS One* **7**, e46678 (2012).
27. L. He, N. Shobnam, W. C. Wimley, K. Hristova, FGFR3 heterodimerization in achondroplasia, the most common form of human dwarfism. *J. Biol. Chem.* **286**, 13272–13281 (2011).
28. M. Terada, A. Shimizu, N. Sato, S. I. Miyakaze, H. Katayama, M. Kurokawa-Seo, Fibroblast growth factor receptor 3 lacking the Ig IIIb and transmembrane domains secreted from human squamous cell carcinoma DJM-1 binds to FGFs. *Mol. Cell Biol. Res. Commun.* **4**, 365–373 (2001).
29. P. L. Toutain, A. Bousquet-Mélou, Plasma terminal half-life. *J. Vet. Pharmacol. Ther.* **27**, 427–439 (2004).
30. A. Bertola, T. Ciucci, D. Rousseau, V. Bourlier, C. Duffaut, S. Bonnafous, C. Blin-Wakkach, R. Anty, A. Iannelli, J. Gugenheim, A. Tran, A. Bouloumié, P. Gual, A. Wakkach, Identification of adipose tissue dendritic cells correlated with obesity-associated insulin-resistance and inducing Th17 responses in mice and patients. *Diabetes* **61**, 2238–2247 (2012).

Acknowledgments: We thank D. Ornitz (Washington University) for providing the *Fgfr3*$^{ach/+}$ mice (*17*) and M. Seo (Kyoto Sangyo University, Japan) for providing the FGFR3ΔTM plasmid (*28*). We thank J. N. Gouze for his wise and helpful comments and his manuscript corrections; V. Corcelle and the C3M Animal Facility team for their valuable assistance with animal care; R. Paul-Bellon for her help with histology; D. Alcor (C3M Imaging Platform) for his expertise and help; J. F. Michiels (Laboratory of Pathological Cytology and Anatomy, L'Archet Hospital) and M. J. Rouby, S. Hivernat, and L. Charpentier for their technical help; C. Sattonnet (Diag/Polyclinique St Jean, Cagnes-sur-Mer) for free access to the SkyScan; and B. Nassar and A. Bros (Biochemistry Laboratory Hospital, Toulouse) for their expertise and technical help, respectively, with biochemical analyses of blood samples. **Funding:** This work was supported by grant PIRG03-GA-2008-226132 from the Marie Curie International Reintegration Grant program within the European Commission FP7-PEOPLE call. B.D. was supported by grant INCA 2010-219 from the French National Cancer Institute (INCA), S.P. by the Fondation pour la Recherche Médicale, and X.M. by the National Research Agency (ANR-2010-EMMA-032-01). This work was also supported by funding from the French National Institute of Health and Medical Research (INSERM) and the University of Nice-Sophia Antipolis (Nice, France). **Author contributions:** S.G. designed and performed the experiments, analyzed the data, performed statistical analyses, and wrote the paper. B.D. performed histology and Western blots and analyzed the data. T.T. analyzed treatment effects on rib cages and performed the proliferation and differentiation studies. N.R. oversaw x-ray analyses, analyzed the data, and edited the manuscript. X.M. performed the CT analysis. S.B. performed the ICW experiments. S.P., a pathologist, analyzed the histological data. A.T. and P.G. analyzed the data and edited the paper. Y.L.M.-B. analyzed the data and wrote the manuscript. I.G. designed and oversaw blood analyses, analyzed the data, and edited the paper. E.G. designed and performed the experiments, analyzed the data, provided supervisory support, and wrote the paper. **Competing interests:** The authors declare that they have no competing interests. **Data and materials availability:** Recombinant FLAG-sFGFR3 is available via material transfer agreement.

Submitted 29 March 2013
Accepted 18 July 2013
Published 18 September 2013
10.1126/scitranslmed.3006247

Citation: S. Garcia, B. Dirat, T. Tognacci, N. Rochet, X. Mouska, S. Bonnafous, S. Patouraux, A. Tran, P. Gual, Y. Le Marchand-Brustel, I. Gennero, E. Gouze, Postnatal soluble FGFR3 therapy rescues achondroplasia symptoms and restores bone growth in mice. *Sci. Transl. Med.* **5**, 203ra124 (2013).

Science Translational Medicine
AAAS

Postnatal Soluble FGFR3 Therapy Rescues Achondroplasia Symptoms and Restores Bone Growth in Mice

Stéphanie Garcia *et al.*

Sci Transl Med **5**, 203ra124 (2013);
DOI: 10.1126/scitranslmed.3006247

Editor's Summary

Receptor Decoy Restores Bone Growth

Achondroplasia is a rare disease where bone growth is stunted and cartilage does not form correctly. It is caused by a mutation in the gene that encodes fibroblast growth factor receptor 3 (FGFR3), which leads to overactive receptor signaling. Yet, despite knowing the cause, a treatment has not been discovered. In an innovative approach, Garcia and colleagues used receptor "decoys" to prevent the FGF ligand from binding its mutated receptor, thus interrupting the signaling cascade and restoring bone growth in mice.

Normal mice or mice with the mutation in the gene encoding FGFR ($Fgfr3^{ach/+}$) were treated with recombinant, soluble FGFR3 (sFGFR3) or a vehicle control for 3 weeks. More than 60% of $Fgfr3^{ach/+}$ mice that were left untreated died during the treatment period, whereas only 12% of sFGFR3-treated mice died from achondroplasia-related complications, such as respiratory distress or paraplegia. In the surviving $Fgfr3^{ach/+}$ animals, those treated with sFGFR3 had normal body and tail lengths, normal rib cage development, and decreased spinal and skull deformities —all similar to their healthy, wild-type counterparts. Untreated transgenic animals suffered from the defects common to achondroplasia: shortened stature, abnormal rib cage structure, and spinal compression, leading to paraplegia and bladder dysfunction.

The sFGFR3 therapy was not toxic to the animals and did not affect reproduction (in fact, by increasing pelvis size in treated transgenic females, litter sizes were normal). Additional preclinical studies will be needed to see if this is a viable long-term treatment for achondroplasia, but with a long half-life and promising early outcomes in animals, this FGFR decoy may be a viable postnatal treatment for translation.

Science Translational Medicine (print ISSN 1946-6234; online ISSN 1946-6242) is published weekly, except the last week in December, by the American Association for the Advancement of Science, 1200 New York Avenue NW, Washington, DC 20005.